# Non-intrusive identification of hydro power plants' dynamics using control system measurements

Sigurd Hofsmo Jakobsen[a],[*], Xavier Bombois[b], Kjetil Uhlen[a]

[a] *Department of Electric Power Engineering, Norwegian University of Science and Technology, Trondheim, Norway*
[b] *Laboratoire Ampère, Ecole Centrale de Lyon, Université de Lyon, Ecully, France*

A B S T R A C T

In this paper we propose two non-intrusive methods for identifying hydro power plant dynamics using standard system identification techniques. The purpose of the tests is to obtain transfer functions relevant for the frequency containment reserves delivered by hydro power plants. To validate the methods, we analytically demonstrate under which conditions the methods will yield consistent results. Moreover, using a simulation example we discuss the validity of the methods when one of the conditions is not met. Results using measurements from the control system of a power plant in the Nordic power system are also provided.

Our proposed methods also allow us to identify a transfer function that can be used to check new requirements developed by the Nordic TSOs. The transfer functions obtained by our methods is compared with the transfer function obtained using the TSOs' methods using Monte Carlo Simulation.

## 1. Introduction

Recent concerns for the frequency quality in the Nordic power system [1] have led to an increased interest in the dynamic performance of the frequency containment process (FCP). This process is responsible for containing frequency deviations and is provided by the frequency containment reserves (FCR). The Nordic transmissions system operators (TSOs) have therefore proposed new requirements for the FCR [2] that include a series of sine tests for estimating the transfer function of the FCR. These tests require disconnection of the plants and may take up to two days. We have therefore investigated less time-consuming and intrusive alternatives, and in this paper we propose two experiments that may serve as non-intrusive alternatives to these tests.

### 1.1. Related work

Traditionally, requirements for hydro power plants are stated in terms of time domain performance, such as in the network codes for grid connection of generators [3]. Following this line of thought [4] proposes a prototype transfer function for checking time domain requirements for hydro power plants. A similar approach is taken in [5], where system identification is used for checking the performance of a steam turbine.

Tests similar to those proposed by the TSOs are often referred to as field tests, which are tests performed while the plant is operating in an open loop. In the paper [6] field tests are used to tune parameters in simulation models based on load rejection tests and steady state

measurements. The paper [7] describes how a model of the turbine can be obtained using a gradient-based non-linear search algorithm fitting measured frequency responses from injection of sine and square waves to the governor. A similar approach was used in [8], where the servo and turbine dynamics were identified from testing at a power plant. For the system identification they used different techniques such as visual inspection grey box identification and analysis of the plant's response in the frequency domain. In addition it was demonstrated how the backlash, which can be found in some servos, can be identified.

In more recent research there has been an attempt to identify hydro power plant dynamics using phasor measurement units (PMUs). These approaches are promising, especially since they do not require the disconnection of the power plant or any other disturbance to the operation. However, as was shown in [9] the transfer function obtained using these approaches are not exactly those needed for checking the requirements. In [10,11] they use ARX and ARMAX model structures to perform the identification, in [9,12,13] a box–Jenkins structure is used and in [14] time domain vector fitting is used.

Another common method for identifying hydro power plant dynamics using PMU measurements is to use measurements from large power system disturbances. This approach is used in the papers [15–18]. In [15,18] an unscented Kalman filter is used for the identification and in [16] constrained optimisation is used for the identification. An example of how to tune simulation models by comparing simulation results with disturbance recordings can be found in [17]. An obvious drawback of these approaches is that they rely on the occurrence of large disturbances. Moreover, these papers do not provide an

---

[*] Corresponding author.
*E-mail address:* sigurd.jakobsen@sintef.no (S.H. Jakobsen).

analytical analysis of whether or not the methods will yield consistent results.

## 1.2. Contributions and outline

To date, research has focused on how best to identify the dynamics without disturbing the plant operation at all or on field tests. In this paper we will contribute to methods for identifying hydro power plant dynamics by:

1. Proposing two non-intrusive experiments for identifying hydro power plant dynamics relevant for the FCR. The experiments use different measurements available from the plant's control system while the plant is in normal operation with added non-intrusive excitation. The amplitude of the added excitation is in the same order of magnitude as the noise already present in the system and does not require disconnection of the plant, and can thus be considered non-intrusive.
2. Demonstrating that our proposed methods also allow for estimating the transfer function needed to test the new requirements proposed by the Nordic TSOs.
3. Analysing whether or not consistent estimates of the relevant dynamics can be obtained using measurements available during normal operation. Aside from [9], this analysis is lacking in the others papers where closed-loop identification is attempted for identifying hydro power plant dynamics. However, this analysis is crucial for ensuring that the results obtained can be used for validating whether or not a hydro power plant complies with the requirements. Moreover, the analysis allows for further analysing and understanding factors that may negatively affect the results.
4. Discussing the effect of process noise on the consistency of the identification. The discussion uses the analytical insights and is backed up by Monte Carlo simulations.
5. Demonstrating that the PMU approach presented in [9] can be seen as a special case of one of the experiments proposed in this paper without added extra excitation.

The outline of the paper is as follows. In Section 2 the power plant model assumed for the analysis is presented. The transfer functions needed to check the requirements are presented in Section 3 and the experiments for checking them are presented in Section 4. In Section 5 two technical theorems relevant for the two experiments we propose are presented, and used in Section 6 for analysing the identifiability of the different transfer functions using the different experiments. Readers who are not interested in why the identification is possible can skip directly to Section 7, which discusses the results from the analysis and provides some simulation examples to illustrate the main points of the analysis. The results from a real power plant are presented in Section 8. Finally, concluding remarks and further work are outlined in Section 9.

## 2. The power plant model used in the paper

For analysing the identifiability of hydro power plant dynamics we will use the model depicted in Fig. 1. Other models and structures are possible, however, the same analysis performed in this paper could easily be conducted for others structures as well. It is important to note that in our analysis the plant is assumed to be operating within a confined region, such that its behaviour can be described by linear models.

In Fig. 1, we use classical notation. The Laplace transform of a continuous-time signal $x(t)$ is denoted by $x(s)$ and the shift operator for a discrete time signal $x[n]$ is denoted by $z$ ($n$ is the sample number).

In Fig. 1, the (first-order) continuous-time transfer function $G_J(s)$ represents the swing dynamics of the power plant. We will assume this transfer function to be of the form:

$$G_J(s) = \frac{1}{2\mathscr{H}s + K_d} \tag{1}$$

where $\mathscr{H}$ is the inertia constant of the machine and $K_d$ is the speed damping. This transfer function is of crucial importance as it determines the initial change in the electrical angular speed of the machine's rotor $\Delta\omega(t)$ due to changes in the difference between the electric power $\Delta P_e(t)$ and the mechanical power $\Delta P_m(t)$. Further change in the speed of the machine is contained by the controller $G_c$, which is responsible for changing $\Delta P_m(t)$ to maintain the power balance. The controller $G_c$ is here assumed to be a digital PID controller and is therefore represented by a discrete-time transfer function $G_c(z)$. Since the controller is digital, the continuous-time speed $\Delta\omega(t)$ needs to be discretised via a sampling mechanism preceded by an anti-aliasing filter $F_{aa}(s)$. The corresponding discrete-time signal is denoted $y[n]$. The signal $r[n]$ is an excitation signal that can be added for identification purposes; this signal is thus equal to zero in normal operation. The discrete-time output $c[n]$ of the controller is transformed into a continuous-time signal via a zero-order hold (ZOH) mechanism. The resulting continuous-time signal $\Delta u_c(t)$ is applied to the servo $G_s(s)$ which changes the water flow to the turbine $G_t(s)$ by changing the opening of the guide vanes $\Delta g(t)$. The parameter $\rho$ in the model is referred to as the droop and determines the steady state gain of the governor.

In Fig. 1, we also assume that we have a discrete-time measurement $u[n]$ of the (continuous-time) electric power $\Delta P_e(t)$, obtained in a similar manner as $\Delta\omega(t)$.

In our modelling we assume the feedback to the controller to be the rotor's electrical angular speed. Other choices are possible and one common choice is to use the power system's electrical frequency as the feedback signal. Since the machines are synchronous machines the power system's frequency will be very close to the rotor's electrical angular frequency. However, it may vary for faster dynamics and we will therefore restrict our analysis to having the rotor's electrical speed as the feedback signal. The speed is measured by measuring how fast the rotor is rotating and the relation between the rotor's mechanical speed and electrical speed is given by:

$$\Delta\omega(t) \triangleq \frac{p}{2}\Delta\omega_m(t) \tag{2}$$

where $\Delta\omega_m(t)$ is the mechanical speed of the rotor and $p$ is the number of poles in the machine.

For the identification it is very important to know how the systems we want to identify are excited. Since the plant is assumed to use the rotor's electrical angular speed as the feedback signal, the main external excitation will be changes in the electric power at the bus bar. For the active power at the bus bar of a synchronous machine we have the following approximate expression [19]

$$P_e(t) = \frac{3V_t(t)E_a(t)\sin\delta_{Ev}(t)}{X_s} \tag{3}$$

where $V_t(t)$ is the terminal voltage of the machine, is the internal voltage, $\delta_{EV}(t)$ is the angle between the internal voltage angle $\delta(t)$ and the terminal voltage angle $\delta_V(t)$, and $X_s$ is the synchronous reactance. If we linearise (3) we get the following equation

$$\Delta P_e(t) = K_t\Delta V_t(t) + K_E\Delta E_a(t) + K_v\Delta\delta_v(t) + K_{11}\Delta\delta(t) \tag{4}$$

where $K_t, K_E, K_v,$ and $K_{11}$ are linearisation constants. For the identification we need to determine whether or not there is external excitation and if the system is operating in a loop. From (4) we see that $\Delta P_e(t)$, which excites the plant is dependent on the rotor angle $\delta(t)$ of the plant. Moreover, the internal voltage $E_a(t)$ and the terminal voltage $V_t(t)$ are dependent on the rotor angle through the excitation system and the automatic voltage regulator of the plant. Several plants also have power system stabilisers (PSS); these control systems change the electric torque of the generator based on measurements of the plant's speed deviation. Based on the above considerations we will assume the following equation for the electrical power of the power plant.
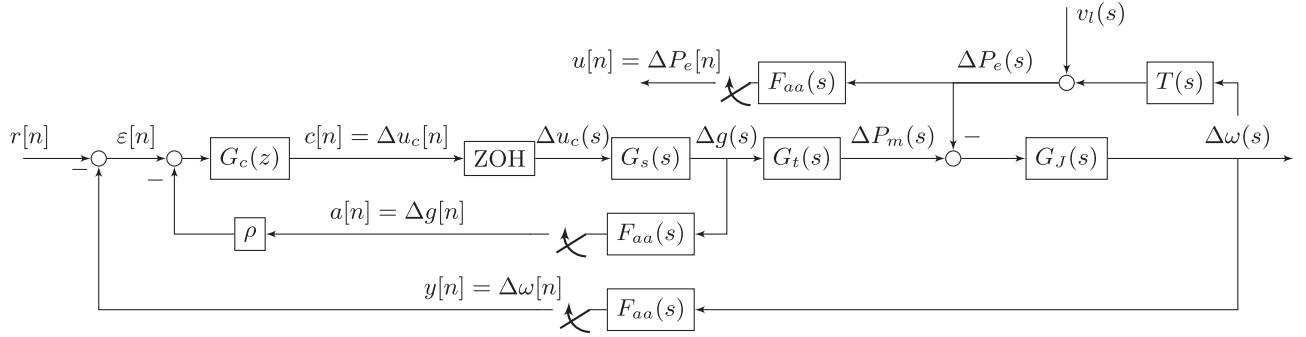
**Fig. 1.** Block diagram of a hydro power plant in a power system.

$$\Delta P_e(s) = v_l(s) + \left(T_v(s) + T_{PSS}(s) + \frac{K_{11}}{s}\right)\Delta\omega(s) = v_l(s) + T(s)\Delta\omega(s) \tag{5}$$

where $v_l(s)$ represents the external excitation provided by random load changes and other random switching events in the power system, $T_v(s)$ is the transfer function from the angular speed of the rotor through the excitation system and voltage regulator to the electrical power, and $T_{PSS}(s)$ is the power system stabiliser. For brevity and since the exact structure of $T_v(s)$ and $T_{PSS}(s)$ is not important for the analysis we will use the transfer function $T(s)$. In Sections 5 and 6, where the identifiability is analysed, we need to know whether or not there is a time delay between the rotor angle $\delta(t)$ and the electrical power $P_e(t)$, from (4) we see that the fourth term $K_{11}\Delta\delta(t)$ represents a direct connection without any time delay.

### 3. Requirements on hydro power plants

In [20] the theory and idea behind the draft requirements are presented. In short they assume that all power plant's can be aggregated to one plant and state stability and performance requirements for this aggregated plant. To check if a plant can fulfill these requirements the power plant owner has to identify the transfer function $G_p(s)$, given in (6), through a series of sine tests, that will be presented in Section 4.

$$G_p(s) = \frac{G_c(s)G_s(s)G_t(s)}{1 + \rho G_c(s)G_s(s)} \tag{6}$$

where $G_c(s)$ denotes the continuous-time equivalent of the digital controller $G_c(z)$. Based on the model of $G_p(s)$, we can directly check the TSO requirements (global/aggregated requirements). In this paper, we will also pay attention to the local stability and performance of the hydro power plant and propose local requirements. For this purpose, let us define two important local transfer functions: the local sensitivity function $S(s)$ and the local plant's disturbance rejection function $G_1(s)$:

$$S(s) = \frac{1}{1 + G_p(s)G_J(s)} \tag{7}$$

$$G_1(s) = G_J(s)S(s) \tag{8}$$

The requirement for the local stability puts a limit on the allowed upper bound $M_s$ for the sensitivity function, that is:

$$\max_{\Omega}\left|S\left(j\Omega\right)\right| < M_s \tag{9}$$

For the local performance requirements it is required to be able to reject a disturbance with a power of $\phi_{P_e}(j\Omega)$ such that the power of the rotor speed is always below a value $\sigma^2_{\omega req}$:

$$\left|G_1\left(j\Omega\right)\right|^2\phi_{P_e}\left(j\Omega\right) < \sigma^2_{\omega req} \tag{10}$$

Another important performance measure of the power plant is the

amount of reserves delivered by the plant. This amount is determined by the droop setting $\rho$ of the plant. In case there is no speed damping and ohmic losses in the turbine and generator, the steady state gain of $G_1(s)$ is given by the droop setting and speed damping of the plant. This means that estimating $G_1(s)$ also gives information on how much FCR a plant can provide given its droop settings.

### 4. Experiments for checking the requirements

In this section we will present the open-loop experiment proposed by the industry and the closed-loop experiments proposed in this paper.

#### 4.1. Description of the industry-proposed experiment

In [2] they propose removing the feedback signal from $y[n]$ to the governor and to identify the transfer function $G_{req}(s)$ between $r[n]$ and $u[n]$ at the frequencies given in Table 1 using (11).

$$G_{req}\left(j\Omega_p\right) = \frac{\mathscr{F}_{\Omega_p}(u[n])}{\mathscr{F}_{\Omega_p}(r[n])} \tag{11}$$

where denotes the value of the discrete Fourier at the frequency $\Omega_p$.

By inspecting Fig. 1 we see that the transfer function $G_{req}(s)$ is given by:

$$G_{req}(s) = \frac{G_p(s)G_J(z)T(s)}{1 + G_J(s)T(s)} \tag{12}$$

For slow dynamics we can neglect the effect of the exciter and voltage regulator, moreover, the PSS is to be disconnected. Consequently, $T(s) \approx K_{11}/s$. If we use this and (1) we can write (12) as

$$G_{req}(s) = \frac{G_p(s)K_{11}}{K_{11} + s(K_d + 2\mathscr{H}s)} \tag{13}$$

The above equation implies that the experiment proposed in [2] identifies $G_p(s)$ through a low pass filter. However, for most practical purposes this should be fine as only slow dynamics are investigated. The time periods investigated are reported in Table 1 and an comparison of $G_{req}(s)$ and $G_p(s)$, using the values for the small power plant in Appendix A, is provided in Fig. 2. In the figure the largest frequency from Table 1 is depicted as the black vertical line. For the power plant in Appendix Appendix A, $G_{req}(s)$ is thus is close to $G_p(s)$ for all the sine tests. However, this cannot in general be guaranteed.

**Remark 1.** The open-loop experiment proposed by the industry to estimate $G_{req}(s)$ will be consistent. For the theory behind open-loop identification, please refer to e.g. [21]. However, it is important to note

**Table 1**
Frequencies of the simulated sine signals.

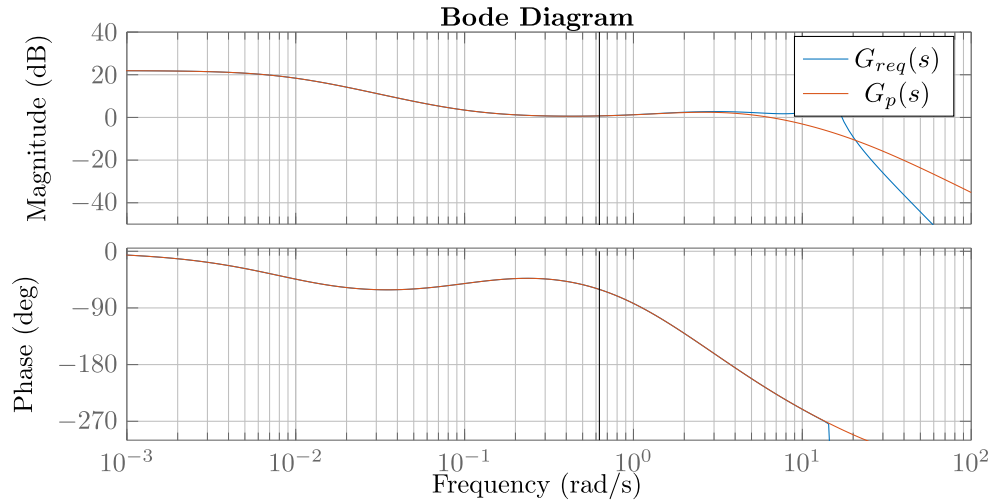| $\frac{2\pi}{300}$ | $\frac{2\pi}{150}$ | $\frac{2\pi}{100}$ | $\frac{2\pi}{80}$ | $\frac{2\pi}{70}$ | $\frac{2\pi}{60}$ | $\frac{2\pi}{50}$ | $\frac{2\pi}{40}$ | $\frac{2\pi}{25}$ | $\frac{2\pi}{15}$ | $\frac{2\pi}{10}$ |
|---|---|---|---|---|---|---|---|---|---|---|

**Fig. 2.** Comparison of $G_p(s)$ and $G_{req}(s)$, the black vertical line corresponds to the largest frequency in Table 1.

that this open-loop experiment is intrusive and does not directly identify the desired transfer function $G_p(s)$.

In the sequel, we present two closed-loop identification approaches. The first method directly yields a model of $S(s)$ and $G_1(s)$ and, from these models, we can derive a model of $G_p(s)$. The second method identifies intermediary models from which models of $S(s)$, $G_1(s)$ and $G_p(s)$ can be deduced.

### 4.2. Experiments proposed in this paper

In this paper we propose using standard system identification techniques for identifying the hydro power plant dynamics while the plant is operating in a closed-loop operation. We will show that these techniques will allow us to derive both a model of $G_p(s)$ (that can be used to verify the industry requirements) and models of $S(s)$ and $G_1(s)$ (that can be used to verify the local requirements discussed in Section 3). To identify these models, we use standard techniques described in [21] and the functions provided by the system identification toolbox available for MATLAB [22]. Since the identification of the transfer functions is performed using a computer, the measured signals will have to be sampled. We will therefore use the discrete version of the signals and transfer functions from now on.

#### 4.2.1. Description of the first closed-loop identification method

By inspecting Fig. 1, we observe that the discrete-time signals $r[n]$, $u[n]$ and $\varepsilon[n] = r[n] - y[n]$ are related by discrete-time versions $S(z)$ and $G_1(z)$ of the continuous-time transfer functions $S(s)$ and $G_1(s)$:

$$\varepsilon[n] = G_1(z)u[n] + S(z)r[n] \tag{14}$$

From this we conclude that if we have collected the dataset $Z_{ur}^N = \{u[n], r[n], \varepsilon[n]|n = 1...N\}$ we can identify $S(z)$ and $G_1(z)$ if the systems are identifiable using this dataset (the identifiability will be the purpose of the next sections). The subscript $ur$ in $Z_{ur}$ denotes the input signals to the multi input single output (MISO) system described by (14). With the models of $G_1(s)$ and $S(s)$, we can check the local requirements of Section 3. From the models of $G_1(s)$ and $S(s)$, we can also deduce a model of $G_p(s)$ using the following relation:

$$G_p(z) = (1 - S(z))G_1(z)^{-1} \tag{15}$$

With the model of $G_p(s)$, we can check the TSO requirements.

Note that if we set $r[n] = 0$, we get the following relation

$$\varepsilon[n] = G_1(z)u[n] \tag{16}$$

In this configuration, it will no longer be possible to identify $S(z)$ and $G_p(z)$. However, it could still be possible to identify $G_1(z)$ using the

dataset $Z_u^N = \{u[n], \varepsilon[n]|n = 1...N\}$

#### 4.2.2. Description of the second closed-loop identification method

We can observe in Fig. 1 that the signals $c[n]$, $u[n]$ and $y[n]$ are related as follows:

$$y[n] = G_{Jp}(z)c[n] - G_J(z)u[n] \tag{17}$$

where $G_J(z)$ is a discretised version of $G_J(s)$ and $G_{Jp}$ is a discretised version of the product $G_s(s)G_t(s)G_J(s)$ (combined with the ZOH and the antia-aliasing filter). We therefore conclude that we could estimate $G_J(z)$ and $G_{Jp}(z)$ using the dataset $Z_{cu}^N = \{c[n], u[n], y[n]|n = 1...N\}$ if the systems are identifiable using this dataset. To find $G_p(z)$ we also need to know the transfer function of the servo $G_s(z)$ and of the controller $G_c(z)$. We will assume the controller to be known and we see that the signals $c[n]$ and $a[n]$ are related by:

$$a[n] = G_s(z)c[n] \tag{18}$$

We therefore conclude that we could estimate $G_s(z)$ using the dataset $Z_c^N = \{c[n], a[n]|n = 1...N\}$ if the system is identifiable using this dataset. An estimate of $G_p(z)$ can then be deduced from the models of $G_J(z)$, $G_{Jp}(z)$, and $G_s(z)$ using the following relation:

$$G_p(z) = \frac{G_{Jp}(z)G_c(z)}{G_J(z)(1 + \rho G_c(z)G_s(z))} \tag{19}$$

The relation (19) allows for checking the TSO proposed requirements. Moreover, we can use the estimates of $G_p(z)$ and $G_J(z)$ and the relations (7) and (8) to derive models of $S(z)$ and $G_1(z)$. With these models, we can check the local requirements of Section 3.

**Remark 2.** For the sequel, it is important to note that the transfer function $G_{Jp}(z)$ will generally contain a delay (due to the presence of the ZOH) while the other transfer functions $G_J(z)$, $S(z)$ and $G_1(z)$ will generally not contain any delay.

### 5. Technical theorems

To prove the identifiability of the systems presented in the previous section we will present two technical theorems: One relevant for MISO systems and one relevant for single input single output SISO systems. In the next section we will then discuss the identifiability of the systems using these theorems.

### 5.1. MISO theorem

We consider the dataset $Z_{miso}^N = \{u_1[n], u_2[n], y[n]|n = 1...N\}$ generated by:

$$\mathscr{S}_{miso}: y[n] = \boldsymbol{G}(z, \theta_0)\boldsymbol{u}[n] + v[n] \tag{20}$$

where $\boldsymbol{G}(z, \theta_0) = [G_1(z, \theta_0) \quad G_2(z, \theta_0)]$ and $\boldsymbol{u} = [u_1[n] \quad u_2[n]]^T$. The term $v[n]$ models process noise and is assumed to be generated by $v[n] = H(z, \theta_0)e[n]$, where $H(z, \theta_0)$ is assumed to be monic and $e[n]$ is white noise with variance $\sigma_e^2$. As we can see in (20) the true system $\mathscr{S}_{miso}$ is parametrised by the parameter vector $\theta_0$. In the sequel, we will suppose that this parameter vector $\theta_0$ is unknown, but that the model structure $\mathscr{M}_{miso} = \{G_1(z, \theta), G_2(z, \theta), H(z, \theta)\}$ is known. Consequently, the identification boils down to the determination of a consistent estimate of $\theta_0$.

The input signals $\boldsymbol{u}^T[n] = [u_1[n] \quad u_2[n]]$ are assumed to be generated with two external excitation signals $w_1[n]$ and $w_2[n]$ and may also be influenced (via some feedback) by the noise $e[n]$ generating $v[n]$ in (20):

$$\boldsymbol{u}[n] = \boldsymbol{K}(z)\boldsymbol{w}[n] + \boldsymbol{\Gamma}(z)e[n] \tag{21}$$

where $w[n] = [w_1[n] \quad w_2[n]]^T$ and where $\boldsymbol{K}(z)$ and $\boldsymbol{\Gamma}(z)$ are a matrix of transfer functions and a vector of transfer functions, respectively. In this paper, we only suppose knowledge of $\boldsymbol{u}[n]$. Consequently, $\boldsymbol{w}[n]$, $\boldsymbol{K}(z)$ and $\boldsymbol{\Gamma}(z)$ are not necessarily known quantities. Using prediction error identification [21] and the dataset $Z_{miso}^N$ an estimate $\widehat{\theta}_N$ of $\theta_0$ can be deduced as follows:

$$\widehat{\theta}_N = \arg\min_\theta \frac{1}{N} \sum_{n=1}^N \epsilon_{miso}^2\left[n, \theta\right] \tag{22}$$

with the prediction error defined as:

$$\epsilon_{miso}[n, \theta] = H^{-1}(z, \theta)(y[n] - \boldsymbol{G}(z, \theta)\boldsymbol{u}[n]) \tag{23}$$

In order to validate our identification setting it is important to verify whether or not (22) and (23) will lead to a consistent estimate of $\theta_0$ when $\boldsymbol{u}[n]$ is generated as in (21). Indeed, if (22) is a consistent estimate of $\theta_0$ and $N$ is sufficiently large, the estimate (22) is normally distributed around $\theta_0$ [21]. The variance of this estimate is then the only source of uncertainty and this variance can be estimated and depends on the number of data $N$ and the excitation signal $u[n]$. To ensure the consistency, we need to verify that the true parameter vector $\theta_0$ is the unique solution to the asymptotic prediction criterion:

$$\theta^* = \arg\min_\theta \overline{E} \, \epsilon_{miso}^2\left[n, \theta\right] \tag{24}$$

with

$$\overline{E} \, \epsilon_{miso}^2\left[n, \theta\right] = \lim_{N\to\infty} \frac{1}{N} \sum_{n=1}^N E \, \epsilon_{miso}^2\left[n, \theta\right] \tag{25}$$

The operator $E$ denotes the expectation operator.

Before we investigate whether or not the estimate (22) is consistent we will make some assumptions.

**Assumption A1.** The external excitations $w_1[n]$ and $w_2[n]$ are assumed to be uncorrelated white noises with variance $\sigma_1^2$ and $\sigma_2^2$ respectively. Moreover, they are assumed to be uncorrelated to the white noise $e[n]$.

**Remark 3.** Other $\boldsymbol{w}[n]$ than white noise could also work, such as multisine and filtered white noise.

**Assumption A2.** The determinant $\det(\boldsymbol{K}(e^{j\Omega}))$ is nonzero for all $\Omega$.

In addition we have the following condition:

**Condition C1.** If we denote $\boldsymbol{\Gamma}(z) = [\Gamma_1(z) \quad \Gamma_2(z)]^T$, there must be a delay in $G_1(z, \theta_0)\Gamma_1(z)$ and in $G_2(z, \theta_0)\Gamma_2(z)$ whenever these transfer functions are nonzero.

The identifiability of the system $\mathscr{S}_{miso}$ is now stated in the following theorem.

**Theorem 1.** *Consider the dataset* $Z_{miso}^N = \{u_1[n], u_2[n], y[n]|n = 1...N\}$ *where* $Z_{miso}^N$ *is generated by* (20) *and* (21). *Moreover, consider Assumptions*

A1 *and* A2 *and Condition* C1 *Then the prediction error criterion* (22) *with* (23) *yields a consistent estimate of* $\theta_0$.

### 5.2. SISO theorem

We now consider the dataset $Z_{siso}^N = \{u[n], y[n]|n = 1...N\}$ generated by:

$$\mathscr{S}_{siso}: y[n] = G(z, \theta_0)u[n] + v[n] \tag{26}$$

where the term $v[n]$ models process noise and is assumed to be generated by $v[n] = H(z, \theta_0)e[n]$, where $H(z, \theta_0)$ is assumed to be monic and $e[n]$ is white noise with variance $\sigma_e^2$ and the input signal $u[n]$ is given by:

$$u[n] = \sum_{i=1}^q K_i(z)w_i[n] + \Gamma(z)e[n] \tag{27}$$

where $q$ is the number of external excitation signals $w_i[n](i = 1...q)$. We observe that $u[n]$ may also be influenced by $e[n]$ via some feedback. As in the previous section, we do not suppose $w_i[n]$, $K_i(z)$ $(i = 1...q)$ and $\Gamma(z)$ to be known. We will nevertheless assume the following:

**Assumption A3.** The signals $w_i[n]$ $(i = 1...q)$ and $e[n]$ are all uncorrelated white noise with variances $\sigma_i^2(i = 1...q)$ and $\sigma_e^2$.

For this system the prediction error is given by:

$$\epsilon_{siso}[n, \theta] = H^{-1}(z, \theta)(y[n] - G(z, \theta)u[n]) \tag{28}$$

In a similar manner to the MISO system we will verify whether or not (28) in (22) can lead to a consistent estimate of $\theta_0$, given the following technical condition.

**Condition C2.** If this transfer function is nonzero, there is a delay in $G(z, \theta_0)\Gamma(z)$.

**Theorem 2.** *Consider the dataset* $Z_{siso}^N = \{u[n], y[n]|n = 1...N\}$ *where* $Z_{siso}^N$ *is generated by* (26) *and* (27) *with* $q \geqslant 1$. *Moreover, consider Assumption* A3 *and Condition* C2. *Then the prediction error criterion* (22) *with* (28) *yields a consistent estimate of* $\theta_0$.

**Remark 4.** For SISO identification, a single external excitation (i.e. $q = 1$) will be sufficient to ensure the consistency. The advantage of having multiple external excitation $(q > 1)$ is the reduction of the variance of the estimate $\widehat{\theta}$.

## 6. Validation of the system identification experiments

### 6.1. Identifiability of $S(z)$ and $G_1(z)$ using the dataset $Z_{ur}^N$

We will now proceed to investigate whether or not the sensitivity function $S(z)$ and the disturbance rejection function $G_1(z)$ can be identified using the dataset $Z_{ur}^N = \{u[n], r[n], \varepsilon[n]|n = 1...N\}$. We assume that the system can be parametrised by a parameter vector $\theta_0$ in a known model structure.

$$\mathscr{S}_{ur}: \varepsilon[n] = G_1(z, \theta_0)u[n] + S(z, \theta_0)r[n] + v[n] \tag{29}$$

where $v[n] = H(z, \theta_0)e[n]$, $e[n]$ is white noise with variance $\sigma_e^2$ and $H(z, \theta_0)$ is assumed to be monic. The term $v[n]$ represents process noise. It is not included in Fig. 1, however, in general it is very unlikely that $\varepsilon[n]$ is perfectly described by (14).

We see that this situation corresponds to the one in Section 5.1 Indeed, by denoting $\boldsymbol{u}^T[n] = [u[n] \ r[n]]$, $\boldsymbol{w}^T[n] = [e_l[n] \ r[n]]$ and by using Fig. 1, we can write the following for some transfer functions $K_{11}(z)$, $K_{12}(z)$ and $\Gamma_1(z)$:

$$\begin{bmatrix} u[n] \\ r[n] \end{bmatrix} = \begin{bmatrix} K_{11}(z) & K_{12}(z) \\ 0 & 1 \end{bmatrix} \begin{bmatrix} e_l[n] \\ r[n] \end{bmatrix} + \begin{bmatrix} \Gamma_1(z) \\ 0 \end{bmatrix} e[n]$$
$$= \boldsymbol{K}(z)\boldsymbol{w}[n] + \boldsymbol{\Gamma}(z)e[n] \tag{30}$$

We observe that, if we apply an excitation signal $r[n]$, we have two external excitation signals generating $\boldsymbol{u}[n] = [u[n] \ \ r[n]]^T$ (i.e. $e_l[n]$ and $r[n]$). Consequently, using Theorem 1, the estimate of $\theta_0$ obtained with prediction error identification using the dataset $Z_{ur}^N$ will be consistent if Assumptions A1, A2 and Condition C1 are fulfilled. Let us discuss this matter in the following remarks:

**Remark 5.** That Assumption A1 does not hold would imply that at least two of the following signals, the aggregated stochastic load behaviour $e_l[n]$, the added perturbation $r[n]$ and the process noise $e[n]$ are correlated. This is highly unlikely.

**Remark 6.** As shown in (30), it is clear that Assumption A2 will always be respected in practice.

**Remark 7.** In this case, Condition C1 boils down to the presence of a delay in $G_1(z, \theta_0)\Gamma_1(z)$. This delay condition does not cause any problems when the feedback mechanism is realised via a digital controller and a ZOH. However, in our case, the feedback mechanism which is at stake in Theorem 1 is the one pertaining to the link between $\Delta\omega(t)$ and $\Delta P_e(t)$. In general, there will be no delay in $G_1(z, \theta_0)\Gamma_1(z)$. Consequently, we will not be able to guarantee the consistency, and the estimate (22) will therefore be biased. However, the bias will remain limited if the contribution of the process noise $v[n]$ in $u[n]$ is negligible. Indeed, in this case, $\nu(z, \theta)$ in (B.4) reduces to $\Delta H(z, \theta)/H(z, \theta)$ and (B.5) holds even if there is no delay in $G_1(z, \theta_0)\Gamma_1(z)$. That the contribution of the process noise $v[n]$ in $u[n]$ is negligible should normally be met in practice as we can expect the contribution of random fluctuations in the rotor angle to influence the power at the bus bar less than the contribution of all other random changes in the power system.

### 6.2. Identifiability of $G_{Jp}(z)$ and $G_J(z)$ using the dataset $Z_{cu}^N$

We will now investigate whether or not we can identify consistent models of $G_{Jp}(z)$ and $G_J(z)$ using the dataset $Z_{cu}^N = \{c[n], u[n], y[n] | n = 1...N\}$, as for the previous system we assume that the system can be parametrised by a parameter vector $\theta_0$ in a known model structure:

$$\mathscr{S}_{cu}: y[n] = \boldsymbol{G}(z, \theta_0)\boldsymbol{u}[n] + v_1[n] \qquad (31)$$

where $\boldsymbol{G}(z, \theta_0) = [G_{Jp}(z, \theta_0) \ \ - G_J(z, \theta_0)]$. The term $v_1[n]$ models process noise and is assumed to be generated by $v_1[n] = H_1(z, \theta_0)e[n]$, where $H_1(z, \theta_0)$ is assumed to be monic. Using Fig. 1, the input signal $\boldsymbol{u}^T[n] = [c[n] \ \ u[n]]$ can thus be rewritten as:

$$\begin{bmatrix} c[n] \\ u[n] \end{bmatrix} = \begin{bmatrix} K_{cl}(z) & K_{cr}(z) \\ K_{ul}(z) & K_{ur}(z) \end{bmatrix} \begin{bmatrix} e_l[n] \\ r[n] \end{bmatrix} + \begin{bmatrix} \Gamma_{ce}(z) \\ \Gamma_{ue}(z) \end{bmatrix} e[n]$$
$$\boldsymbol{u}[n] = \boldsymbol{K}(z)\boldsymbol{w}[n] + \boldsymbol{\Gamma}(z)e[n] \qquad (32)$$

If an external signal $r[n]$ is applied to the system, we are thus here also in a situation corresponding to Section 5.1 and, using Theorem 1, the estimate of $\theta_0$ obtained with the dataset $Z_{cu}^N$ will be consistent if Assumption A1, A2 and Condition C1 are fulfilled. Assumption A1 and A2 are generically fulfilled in this case too. However, we have a similar problem with Condition C1, which requires a delay in both $G_{Jp}(z, \theta_0)\Gamma_{ce}(z)$ and $G_J(z)\Gamma_{ue}(z)$, as discussed in the following remark:

**Remark 8.** The delay condition will generally hold for $G_{Jp}(z, \theta_0)\Gamma_{ce}(z)$ due to the presence of the ZOH (see Remark 2). However, for the same reason as in Remark 7, this will not be the case for $G_J(z, \theta_0)\Gamma_{ue}(z)$. The undesired bias will however be limited under the same condition as in Remark 7.

### 6.3. Identifiability of $G_1(z)$ without external excitation using dataset $Z_u^N$

We will now investigate whether or not $G_1(z)$ can be identified without adding external excitation, i.e. $r[n] = 0$. This possibility was

mentioned in Section 4.2.1 (see (16)). Note that we analysed this particular case in a previous paper[9], but it will also be included here for the sake of completeness with extra attention given to the delay condition. As for the previous system we assume that $G_1(z)$ can be parametrised by a parameter vector $\theta_0$ in a known model structure. The relevant dataset for this analysis is $Z_u^N = \{u[n], \varepsilon[n] | n = 1...N\}$, which we suppose is generated by:

$$\mathscr{S}_u: \varepsilon[n] = G_1(z, \theta_0)u[n] + v[n] \qquad (33)$$

and using (30) with $r[n] = 0$. We are thus now in the situation described in Section 5.2 with $q = 1$. Consequently, using Theorem 2, the estimate of $\theta_0$ obtained with the dataset $Z_u^N$ when $r[n] = 0$ will be consistent if $e_l[n]$ is independent of $e[n]$ (Assumption A3) and if Condition C2 holds. This latter condition here entails the presence of a delay in $G_1(z, \theta_0)\Gamma_1(z)$. As already mentioned in Remark 7, this will not be the case in practice, but the bias will be limited under the same condition as the one mentioned in Remark 7.

**Remark 9.** If we are only interested by $G_1(z, \theta_0)$, it is thus not necessary to add the external excitation $r[n]$. However, as pointed out in Remark 4 adding this external excitation $r[n]$ and following the procedure in Section 6.1 will generally yield an estimate with lower variance. The addition of an external excitation $r[n]$ will also make it more likely that the contribution of $v[n]$ in $u[n]$ is negligible, reducing in this way the bias due to the absence of delay in $G_1(z, \theta_0)\Gamma_1(z)$ (see Remark 7).

### 6.4. Identifiability of $G_s(z)$ using the dataset $Z_c^N$

We will now investigate whether or not we can identify $G_s(z)$. For this purpose, we assume that the system can be parametrised by a parameter vector $\theta_0$. The relevant dataset in this case $Z_c^N = \{c[n], a[n] | n = 1...N\}$ is supposed generated by:

$$\mathscr{S}_c: a[n] = G_s(z, \theta_0)c[n] + v_2[n] \qquad (34)$$

$v_2[n]$ models process noise and is assumed to be generated by $v_2[n] = H_2(z, \theta_0)e_2[n]$, where $H_2(z, \theta_0)$ is assumed to be monic. It is arguable whether there will be significant process noise in the servo; however, it is included for completeness and it will be supposed that this signal $v_2$ is uncorrelated with $e_l[n]$ and $v[n]$. The signal $v_2[n]$ will generally be negligible in practice with respect to $e_l[n]$ and $v[n]$. That is the reason why it was not considered as an extra external excitation in the previous subsection. The signal $c[n]$ in (34) will be made up of a contribution of the random load changes $e_l[n]$, the process noise $e[n]$ and possibly of a contribution of the external excitation $r[n]$.

This situation corresponds to the case discussed in Section 5.2. Using Theorem 2, this identification will therefore yield a consistent estimate since all conditions/assumptions are here respected. In particular, note that, here, Condition C2 will hold since the to be identified transfer function $G_s(z, \theta_0)$ will generally contains a delay (due the presence of the ZOH between $c[n]$ and $a[n]$).

Note also that, due to the presence of $e_l[n]$, we will necessarily have $q \geqslant 1$ and the external excitation $r[n]$ is thus not required for the consistency.

## 7. Simulation results and discussion

We will now proceed with a numerical example.

### 7.1. Simulation set up

For the simulations, the simple test system depicted in Fig. 3 was implemented in Simulink. The power plants at bus 1 and 2 were modeled using their synchronous reactance, the swing equation, the non-linear model assuming a non-elastic water column described in [23] for the turbine and governor. For the plant at bus 1 the governor from [23] was replaced with a digital PI regulator. A DC power flow
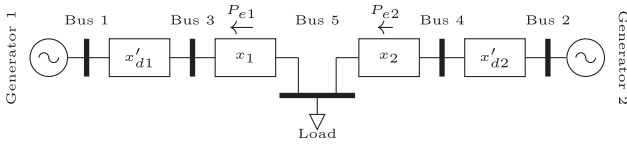
**Fig. 3.** Small test system used for the simulations.

was used for modelling the power flow. The stochastic load at bus 5 was modelled as white noise through an integrator. Its power was chosen such that the power system frequency stayed within its allowed band of $0.1Hz$. Process noise was added to the angular speed $\Delta\omega[n]$ of the power plant at bus 1. For a more detailed derivation of the test system please refer to [24]. When $r[n] = 0$ the only external excitations are $e[n]$ and $e_l[n]$, which means that no process noise is added to the power plant at bus 2. In this section, the excitation signal $r[n]$ will always be applied and will be given by a white noise of standard deviation $\frac{0.1}{50\cdot3}$. This standard deviation was chosen to keep the per-unit value of $r[n]$ within $0.1[Hz]$ with a 99.7% probability, where $0.1/50[p.u.]$ is the allowed band of the power system frequency in normal operation[1].

To strengthen the conclusions from the simulations a Monte Carlo Simulation (MCS) approach was used. The approach consisted of running the test system for a simulation time of $1800s$ to generate the different datasets. The transfer functions $S(z, \hat{\theta}_N)$, $G_1(z, \hat{\theta}_N)$, $G_p(z, \hat{\theta}_N)$ and $G_J(z, \hat{\theta}_N)$ were then identified using these datasets and the functions provided by the system identification MATLAB toolbox [22]. For the SISO systems a box–Jenkins model structure was used and for the MISO systems a high-order ARX model structure was preferred. These simulations and identification were repeated a 1000 times, and stochasticity was added by regenerating the process noise $e[n]$, and the stochastic load $e_l[n]$ after each simulation. Since $r[n]$ is a signal generated for the purpose of the identification it is only generated once.

As mentioned in Remarks 7–9, the absence of a delay in certain transfer functions leads to a bias that will be smaller for larger values of the signal to noise ratio (SNR) (by SNR, we here mean the ratio of the contribution of $e_l[n]$ and $r[n]$ to $u[n]$). To check this, we ran multiple MCS for different values of the SNR. Different SNR values can be obtained by changing the variance of $e[n]$ in the process noise. The lowest SNR we tried was $0dB$, which means that random fluctuations in the angular speed of the machine contributes equally to the measured electric power as random power fluctuations due to load and other switching events in the power system.

### 7.2. The influence of process noise on the identification using $Z_{cu}^N$

Let us first consider the experiment of Section 4.2.2 and let us apply this experiment 1000 times and for different values of the SNR to derive models for $G_p(z)$ and $G_J(z)$. These models of $G_p(z)$ and $G_J(z)$ can subsequently be used to derive models for $G_1(z)$ and $S(z)$ using (7) and (8).

In Fig. 4, we represent the means of the frequency responses of the models $G_p(z)$ and $G_J(z)$ obtained in this way and we observe that the bias remains limited. The same can also be said for the means of the models for $G_1(z)$ and $S(z)$ (see Figs. 5 and 6).

### 7.3. The influence of process noise on the identification using $Z_{ur}^N$

The procedure of Section 4.2.1 based on the dataset $Z_{ur}^N$ has also been tested using a MCS for different values of the SNR. This procedure yields the mean values represented in blue in Figs. 5 and 6. We observe a larger bias than in the case of the procedure in Section 4.2.2, especially for the low frequency range of $S(z)$. The procedure in Section 4.2.1 thus appears more sensitive (at least in this example) to the bias introduced by the absence of delay. Note also that, since $S(z)$ is

identified directly in this procedure, the low gain in low frequencies is more difficult to identify (see Fig. 5).

### 7.4. Checking the requirements using the different experiments

We will now proceed to compare which method is best for checking the different parts of the local requirements described in Section 3. To perform the comparison we will use a normalised root mean square error (NRMSE) defined as follows:

$$NRMSE = \sqrt{\frac{1}{L}\frac{\sum_{i=1}^{L}(a_0 - a_i)^2}{a_0^2}} \tag{35}$$

where $a_0$ is the true value of the quantity to be estimated, $a_i$ is the estimate of $a_0$ obtained at MCS iteration $i$, and $L$ is the number of MCS iterations.

In Fig. 7 the different identification methods that yield a model of $G_1(z)$ and that therefore allow us to check the local performance requirement given in (10) are compared. In the comparison we look at the peak and steady state gain of the estimated transfer function. The steady state gain of $G_1(z)$ is of interest since it is closely related to the droop setting $\rho$ of the plant, which is how much FCR the plant is providing. It should be noted that checking the peak of $G_1(z)$ is only sufficient if $P_{e1}[n]$ is white noise. However, since the true nature of $P_{e1}[n]$ may vary from system to system we chose in this case to look at the peak.

In Fig. 7a the NRMSE results for the different identification methods (i.e. the ones using $Z_{cu}^N$, and $Z_{ur}^N$) are presented for the case where $a_0$ in (35) is the true value of the steady state gain $G_1(z = 1)$ of $G_1(z)$. Note that this true value is $G_1(z = 1) = 0.0794$. From this figure, it can be concluded that the best experiment to use for our simulation setup is the dataset $Z_{cu}^N$.

In Fig. 7b the same datasets are used to compare which dataset is best for estimating $\max_\Omega|G_1(e^{j\Omega})| = 1.01$. The dataset $Z_{cu}^N$ clearly gives best results and is less sensitive to the SNR change.

Let us now consider the second local performance requirement, i.e. the one linked to $S(z)$. As shown in (9), we are here only interested in the peak gain which, in our example, is equal to 1.29. The two methods allowing us to identify $S(z)$ (i.e. the ones using $Z_{ur}^N$ and $Z_{cu}^N$) are evaluated in Fig. 8 in their ability at estimating this peak gain. Just as with the peak gain of $G_1(z)$ the dataset $Z_{cu}^N$ provides the best results.

### 7.5. Comparison with industry-proposed experiment

We also tested the industry-proposed experiment using the described MCS approach. To do this, let us consider the following NRMSE that will be defined at all frequencies of Table 1:

$$NRMSE(\Omega) = \sqrt{\frac{1}{L}\frac{\sum_{i=1}^{L}\left|G_p(e^{j\Omega}) - G_i(e^{j\Omega})\right|^2}{|G_p(e^{j\Omega})|^2}} \tag{36}$$

where $G_p(e^{j\Omega})$ is the frequency response at $\Omega$ of $G_p(z)$. For the closed-loop method of this paper (we will here only consider the method using $Z_{cu}^N$), $G_i(e^{j\Omega})$ is directly the model of $G_p(e^{j\Omega})$ obtained at MCS iteration $i$. For the industry-proposed method, $G_i(e^{j\Omega})$ is the estimate of $G_{req}(e^{j\Omega})$ obtained at MCS iteration $i$ (see Section 4). In (36), $|x|$ is the modulus of the complex number $x$.

Fig. 9 gives the corresponding results. From the figure it can be seen that the NRMSE increases for both experiments with increasing frequencies. Our closed-loop approach performs similarly to the industry-proposed approach. The industry-proposed approach seems less sensitive to the noise in our setup. However, to determine which test is best in practice, actual SNR levels from real power plants must be investigated.

---

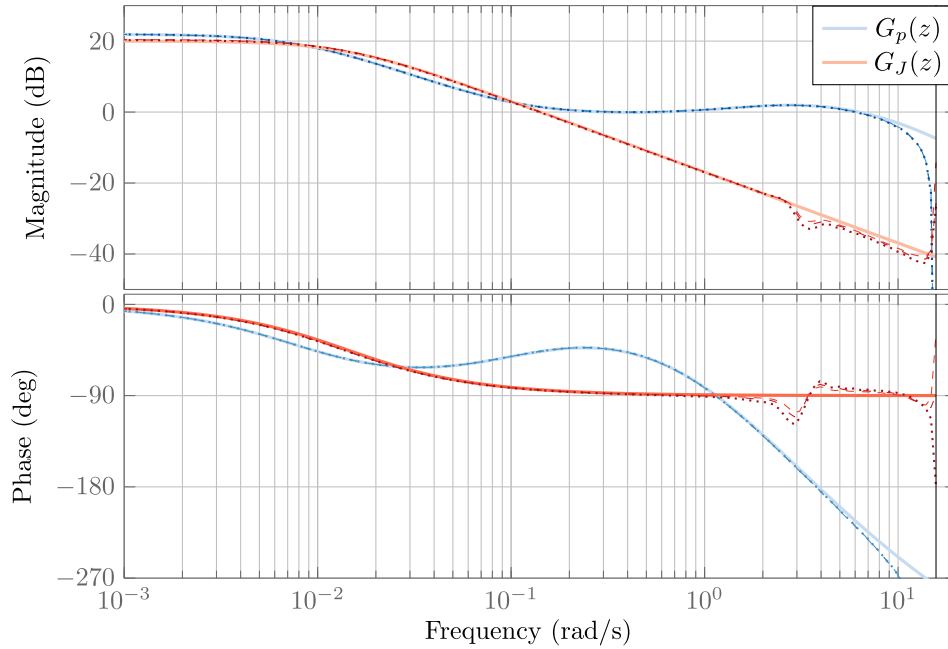[1] In practice the power system will sometimes leave this band.

**Fig. 4.** The mean value of $G_p(z, \hat{\theta}_N)$ and $G_J(z, \hat{\theta}_N)$ calculated from the MCS. The solid lines are the analytical calculated versions and the dashed, loosely dashed, and dotted lines represent an SNR of $12dB$, $6dB$, and $0dB$ respectively.
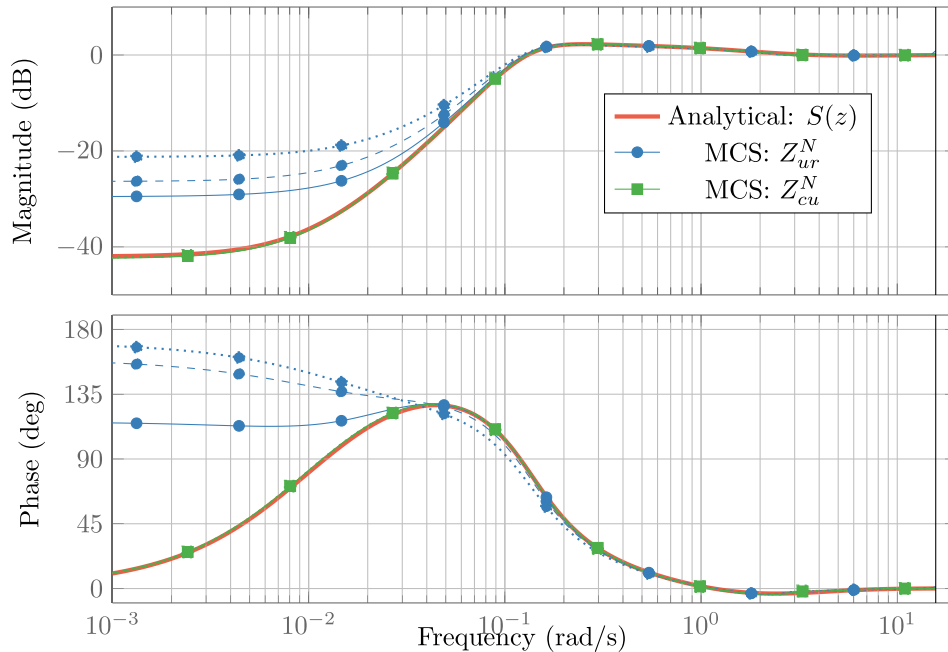


**Fig. 5.** The mean value of $S(z, \hat{\theta}_N)$ calculated from the MCS with different levels of SNR compared to the analytical calculated $S(z)$. The solid, dashed and dotted lines represent an SNR of $12dB$, $6dB$, and $0dB$ respectively.

Fig. 9 (and the previous figures) has been obtained for a dataset of length 30 min. For the industry method, since an experiment has to be performed for every frequency in Table 1, this means that the total experiment duration is 330 min. Consequently, the industry-proposed experiment is very time-consuming with respect to the method proposed in this paper for which the experiment duration is just 30 min. An experiment duration of 330 min may be deemed too long for the intrusive industry method. Let us thus also evaluate its performance and that of the closed-loop method for a dataset length of 10 min. In Fig. 10, the different experiments with a dataset length of 10 min and varying levels of SNR are depicted. In this case we see that our closed-loop approach performs better for all considered SNR.

Until now, we have supposed that we have an exact measurement of the electrical power $u[n]$. Since this quantity will be measured with a sensor, a measurement error will nevertheless always be present. In the industry-proposed method, $u[n]$ is the output of the to-be-identified system. Consequently, the measurement error will increase the variance of the estimate. In our closed-loop apporaches, $u[n]$ is considered as an input of the to-be-identified system and the identification problem is then a so-called error-in-the-variable problem [21], which could in theory be more problematic. It is therefore important to investigate what are the consequences of a reasonable measurement error on $u[n]$ for the industry-based method and for the prefered closed-loop method (the one based on the data set $Z_{cu}^N$) when, in both approaches, we will
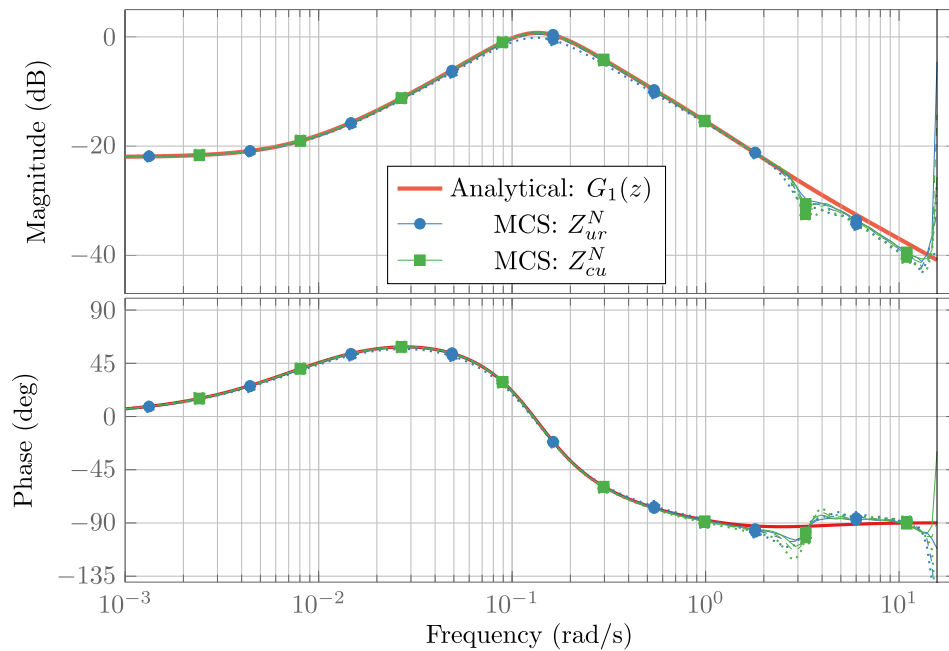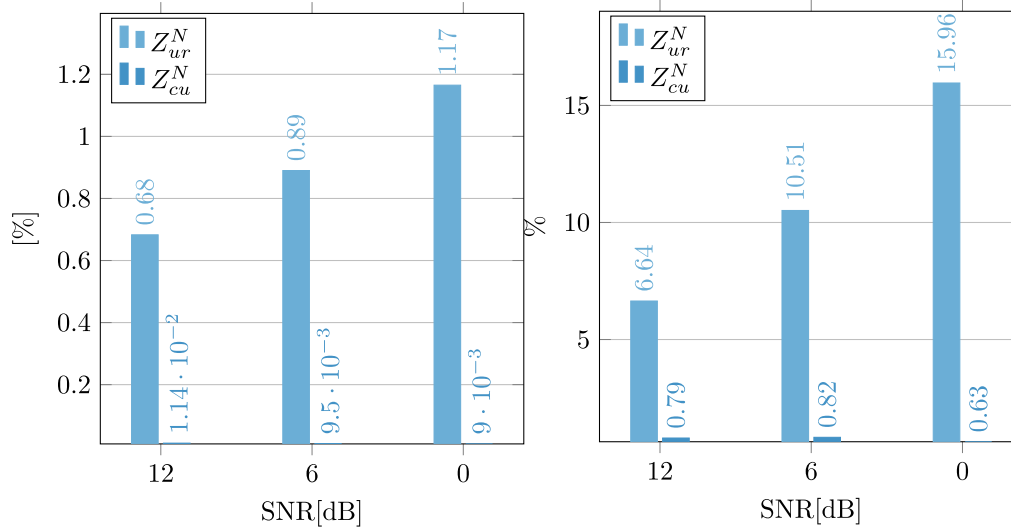
Fig. 6. The mean value of $G_1(z, \hat{\theta}_N)$ calculated from the MCSwith different levels of SNR compared to the analytical calculated $G_1(z)$. The solid, dashed and dotted lines represent an SNR of $12dB$, $6dB$, and $0dB$ respectively.



(a) NRMSE of $\lim_{z \to 1} |G_1(z)|$ calculated from MCS.

(b) NRMSE of $\max_\Omega |G_1(e^{j\Omega})|$ calculated from the MCS.

Fig. 7. Comparison of different methods for checking the requirements for local performance.

use the measured signal $u[n]$ for the identification. In a power plant the electric power used by the control system is obtained using voltage and current measurement transformers. The maximum allowed measurement error for the different accuracy classes for measurement transformers defined in [25], close to rated power, are in the range 0.15% to 1.2%. In Fig. 11 we compare results obtained using the dataset $Z_{cu}^N$ and the industry-proposed method with different levels of process noise and a measurement noise level of 1%. When comparing Fig. 9 (obtained with no measurement noise) and Fig. 11 (obtained with 1% measurement noise), we can conclude that the measurement error that is typicalled observed in practice hardly modifies the results in this example.

**8. Results from a real power plant**

In this section, the procedure discussed in Section 6.3 (i.e. a

procedure with $r[n] = 0$) will be used on real-life data. A test was performed on a power plant in the Norwegian power system. For the test the dataset $Z_u^N$ was collected with a small adjustment with respect to Fig. 1: the plant was operating with the power system frequency as the feedback signal. It would be possible to operate with the angular speed of the rotor as the feedback signal. However, to change to this operation the plant would have to be shut down. Since the difference between these two signals is negligible for slow dynamics, we decided not to change the feedback signal.

The results obtained from five different datasets are depicted in Fig. 12. The identified transfer functions are plotted together with their 95% confidence interval, which is added to the figure as lines with some opacity. The droop constant $\rho$ was chosen differently in each of these datasets. Moreover, the proportional constant of the PID regulator was changed from 2.5 to 5 for the datasets where the droop was below 6%.
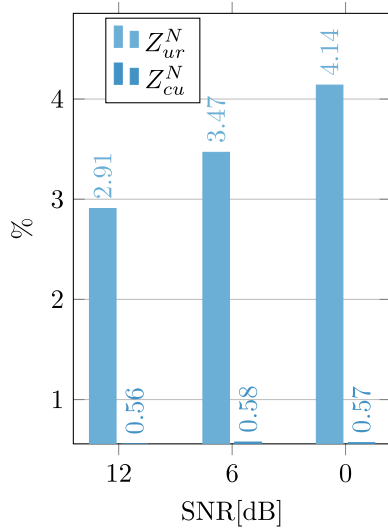
**Fig. 8.** NRMSE of $\max_\Omega |S(e^{j\Omega})|$ calculated from the MCS.

The parameters were changed at intervals of one hour and the datasets were recorded in between, so the datasets are about an hour long. In the figure it can clearly be seen that the static gain of the disturbance rejection is changed when the droop is changed. Similarly, a change in the peak of the transfer function can clearly be seen when the proportional constant of the PID regulator is changed. The legend of Fig. 12 shows the value of the droop the plant owner used for the dataset.

To determine the accuracy of the obtained estimate, the droop

setting was compared with the one calculated from the steady state gain of the estimated transfer function. The results are presented in Table 2. As can be seen from the table there is a good correspondence even when only a part of the full dataset (of 60 min) is used for the identification.

## 9. Concluding remarks and further work

The Nordic TSO have developed draft requirements for the FCR providers that require open-loop testing of the plants. In this paper we have proposed two non-intrusive alternative experiments. These experiments have the added benefit of identifying the transfer functions relevant for the local plant stability and performance.

We have shown that the dynamics relevant for the local stability and performance of the FCP of a hydro power plant can be identified in closed loop operation if extra excitation is added. Although, consistency cannot in general be guaranteed, due to the lack of a time delay, we expect potential bias due to the lack of time delay to be negligible. This was demonstrated by testing the identification procedure with large levels of process noise. Moreover, the local performance ($G_1(z)$) can be checked without adding extra excitation. The best results were obtained by using the dataset $Z_{cu}^N$; That is to say, by measuring the output from the PI controller, the electric power and angular speed of the rotor.

Our experiment using the dataset $Z_{cu}^N$ were also compared to the experiment proposed by the TSOs. This comparison showed that the experiment proposed by the TSOs were less sensitive to the levels of process noise we tested with. However, our proposed experiment estimated $G_p(z)$ better than the TSO propsed experiment for most of the levels of the process noise, and our method was better with shorter dataset lengths. With respect to measurement noise the dataset $Z_{cu}^N$ gave similar results as the TSO proposed experient.
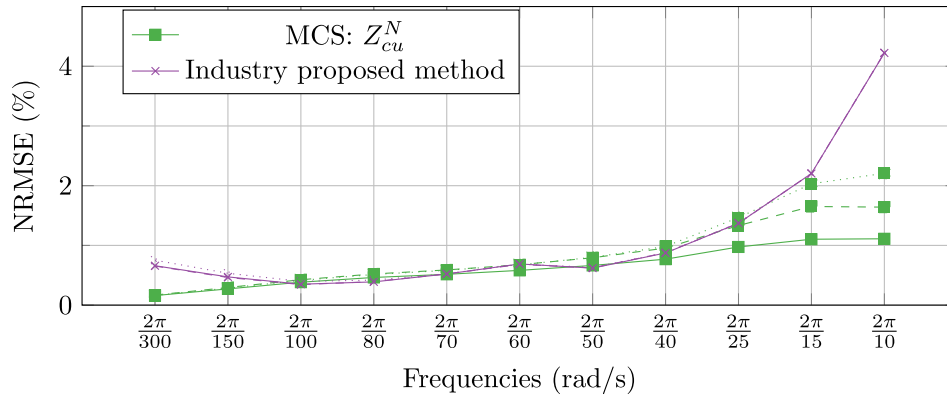


**Fig. 9.** NRMSE (36) with different levels of SNR with dataset lengths of 30 min. The solid, dashed and dotted lines represent an SNR of $12dB$, $6dB$, and $0dB$ respectively.
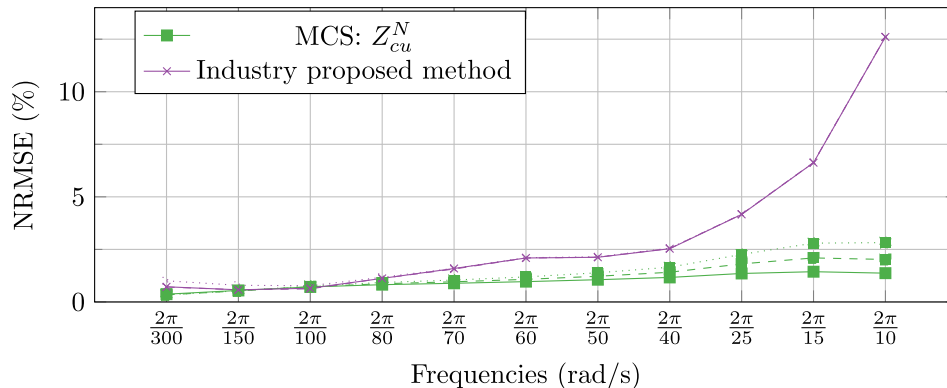


**Fig. 10.** NRMSE (36) with different levels of SNR with dataset lenghts of 10 min. The solid, dashed and dotted lines represent an SNR of $12dB$, $6dB$, and $0dB$ respectively.
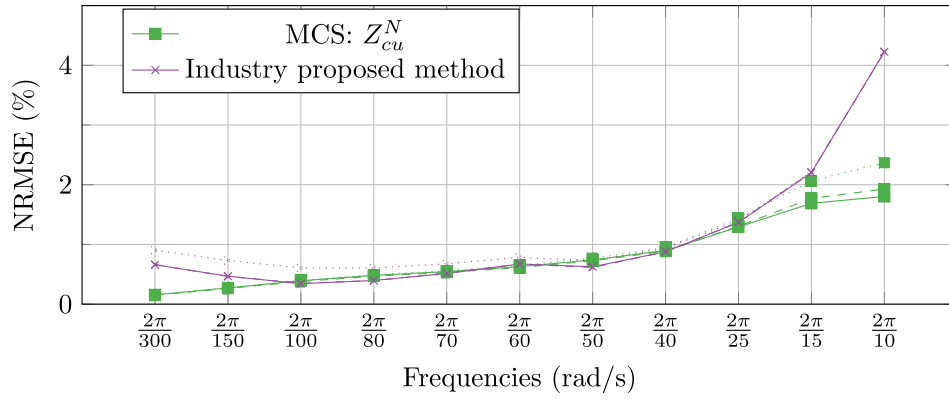
**Fig. 11.** NRMSE (36) with different levels of SNR with dataset lengths of 30 min and a measurement noise level of 1%. The solid, dashed and dotted lines represent an SNR of $12dB$, $6dB$, and $0dB$ respectively.

In addition to the analytical insight and the simulation examples, some results from a real power plant were also presented. These results were obtained without adding extra excitation and therefore could only be used for identifying $G_1(z)$. The results were promising and we demonstrated that the method could estimate the droop setting of the machine and detect changes in the PID parameters.

Although the presented results from a real power plant are promising, more tests should be conducted on real power plants. This paper demonstrates that alternative experiments are possible; however, it still remains to investigate whether or not the process noise will be a problem in real power plants and if it can be mitigated. It should also be investigated for what types of power plants backlash is a problem and how to mitigate it. In Pelton turbines there is normally no backlash; however, it is a well-known fact that this may not be the case for high-pressure Francis turbines and Kaplan turbines.

In conclusion we have shown both analytically and using simple simulation examples that it is possible to check the new requirements using non-intrusive experiments. Indeed, it is even possible to identify the turbine and swing dynamics of the plant in addition to the FCP dynamics using the non-intrusive experiments. We have also shown

**Table 2**
Droop setting and $\lim_{z\to 1}|G_1(z)|$.

| Droop | Dataset lenght | | | |
|---|---|---|---|---|
| | 60 min | 45 min | 30 min | 15 min |
| 10% | 9.5% | 9.5% | 9.5% | 9.5% |
| 6% | 6.2% | 6.0% | 5.9% | 6.1% |
| 5% | 4.9% | 4.9% | 5.0% | 5.1% |
| 3% | 3.1% | 3.1% | 3.1% | 2.9% |
| 2% | 2.0% | 1.8% | 1.8% | 1.7% |

that the results using our method were similar in accuracy to those of the experiment proposed by the TSO, even with considerable levels of process noise. Our method also only requires one dataset and works well with short datasets. It should therefore be of interest as an alternative for the TSO-propsed method that requires 11 datasets. However, to determine the most accurate and suitable method, more tests should be conducted at actual power plants.
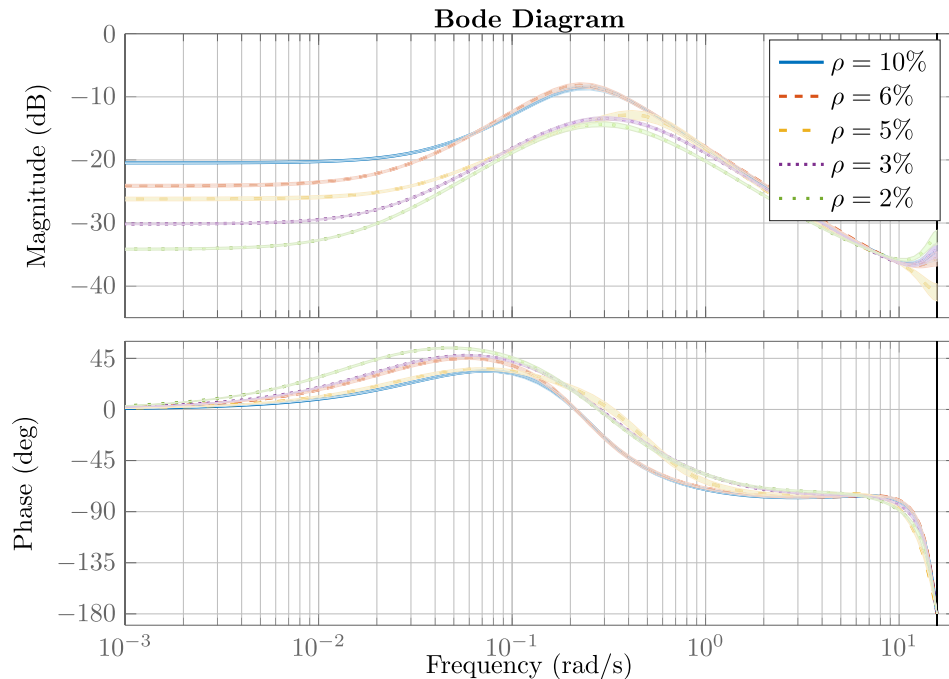


**Fig. 12.** Identification of $G_1(z, \hat{\theta}_N)$ with different droop.

## Declaration of Competing Interest

The authors declare that they have no known competing financial interests or personal relationships that could have appeared to influence the work reported in this paper.

## Appendix A. Simulation parameters

See Tables A.3–A.5.

**Table A.3**
The parameters used for Fig. 3.

| Variable | Explanation | Value | |
|---|---|---|---|
| $S_1$ | Machine 1 base power | 300 MW | - |
| $S_2$ | Machine 2 base power | 3 GW | - |
| $S_{base}$ | System base power | 3.3 GW | - |
| $U_{base}$ | Base voltage for the transmission system | 400 kV | - |
| $U_M$ | base voltage for the machines | 20 kV | - |
| $D$ | Proportional load frequency dependency | 50 | $S_{base}$ |
| $H_1$ | Generator 1 inertia constant | 3.5 | |
| $H_2$ | Generator 2 inertia constant | 9.60 s | |
| $K_{d1}$ | Damping constant | 0.1 | - |
| $k_{d2}$ | Damping constant | 0.1 | - |
| $x_1$ | Reactance between bus 3 and 5 | 1 | $S_{base}$ |
| $x_2$ | Reactance between bus 4 and 5 | 1 | $S_{base}$ |
| $x_{d1}$ | Sub transient reactance generator 1 | 0.15 | $S_1$ |
| $x_{d2}$ | Sub transient reactance generator 2 | 0.15 | $S_2$ |

**Table A.4**
Hydro turbine governor parameters plant 1.

| Variable | Explanation | Value |
|---|---|---|
| $T_f$ | Low pass filter time constant | 0.05 s |
| $K_p$ | PI proportional constant | 1 |
| $T_i$ | PI integral time | 9.1 s |
| $\rho$ | Droop | 0.08 |
| $T_g$ | Servo time constant | 0.2 s |
| $T_w$ | Water starting time | 1 s |
| $q_{nl}$ | No load flow | 0.1 |
| $h_s$ Static head of water column | 1 | |
| $A_t$ Turbine gain | 1 | |

**Table A.5**
Hydro turbine governor parameters plant 2.

| Variable | Explanation | Value |
|---|---|---|
| $T_f$ | Low pass filter time constant | 0.05 s |
| $T_r$ | Droop time constant | 5 s |
| $r$ | Temporary droop | 0.3 |
| $\rho$ | Droop | 0.08 |
| $T_g$ | Servo time constant | 0.2 s |
| $T_w$ | Water starting time | 1 s |
| $q_{nl}$ | No load flow | 0.1 |
| $h_s$ Static head of water column | 1 | |
| $A_t$ Turbine gain | 1 | |

## Appendix B. Proof of the technical theorems

### B.1. Proof of Theorem 1

**Proof.** We start by inserting (20) into (23) to obtain:

$$\epsilon_{miso}\left[n, \theta\right] = e[n] + \frac{\Delta G(z, \theta)u[n] + \Delta H(z, \theta)e[n]}{H(z, \theta)}$$

(B.1)

with $\Delta G(z, \theta) = G(z, \theta_0) - G(z, \theta)$ and $\Delta H(z, \theta) = H(z, \theta_0) - H(z, \theta)$. We now insert (21) into (B.1).

$$\epsilon_{miso}[n, \theta] = e[n] + \nu(z, \theta)e[n] + \chi(z, \theta)\boldsymbol{K}(z)\boldsymbol{w}[n] \tag{B.2}$$

with

$$\chi\left(z, \theta\right) = \frac{\boldsymbol{\Delta G}(z, \theta)}{H(z, \theta)} \tag{B.3}$$

and

$$\nu\left(z, \theta\right) = \chi\left(z, \theta\right)\begin{bmatrix} \Gamma_1(z) \\ \Gamma_2(z) \end{bmatrix} + \frac{\Delta H(z, \theta)}{H(z, \theta)} \tag{B.4}$$

Due to the monicity of $H(z, \theta_0)$ and the combination of Assumption A1 and Condition C1, we have that:

$$\overline{E} \ \epsilon_{miso}^2[n, \theta] = \sigma_e^2$$
$$+ \frac{1}{2\pi} \int_{-\pi}^{\pi} \nu(e^{j\Omega}, \theta)\sigma_e^2\nu(e^{-j\Omega}, \theta)d\Omega$$
$$+ \frac{1}{2\pi} \int_{-\pi}^{\pi} \chi(e^{j\Omega}, \theta)\boldsymbol{\phi}_{\boldsymbol{Kw}}(\Omega)\chi^T(e^{-j\Omega}, \theta)d\Omega \tag{B.5}$$

with

$$\boldsymbol{\phi}_{\boldsymbol{Kw}}(\Omega) = \boldsymbol{K}(e^{j\Omega})\boldsymbol{\phi}_w(\Omega)\boldsymbol{K}^T(e^{-j\Omega}) \tag{B.6}$$

where $\boldsymbol{\phi}_w(\Omega) = diag(\sigma_1^2, \sigma_2^2)$. Let us first observe that (B.6) is a strictly positive definite matrix at each $\Omega$ by Assumption A2. To prove the consistency, we will show that $\theta_0$ is the unique minimszer of (B.5). That is to say, it is the unique parameter vector $\theta^*$ yielding $\overline{E} \ \epsilon_{miso}^2[n, \theta^*] = \sigma_e^2$. Since (B.6) is strictly positive definite, we observe that this only holds if $\chi(\theta^*) = \nu(\theta^*) = 0$ for all $\Omega$. From (B.3) and (B.4), this implies that $\boldsymbol{\Delta G}(\theta^*) = \Delta H(\theta^*) = 0$ for all $\Omega$; which in turn implies $\theta^* = \theta_0$. $\square$

## B.2. Proof of Theorem 2

**Proof.** We start by inserting (26) into (28) to obtain.

$$\epsilon_{siso}[n, \theta] = e[n]$$
$$+ \frac{\Delta G(z, \theta)u[n] + \Delta H(z, \theta)e[n]}{H(z, \theta)} \tag{B.7}$$

with $\Delta G(z, \theta) = G(z, \theta_0) - G(z, \theta)$, and $\Delta H(z, \theta) = H(z, \theta_0) - H(z, \theta)$.

Due to the monicity of $H(z, \theta_0)$ combined with Assumption A3 and Condition C2,

$$\overline{E} \ \epsilon_{siso}^2[n, \theta] = \sigma_e^2 + \frac{1}{2\pi} \int_{-\pi}^{\pi} \zeta(e^{j\Omega}, \theta)\sigma_e^2\zeta(e^{-j\Omega}, \theta)d\Omega$$
$$+ \frac{1}{2\pi} \sum_{i=1}^{q} \int_{-\pi}^{\pi} \chi_i\left(e^{j\Omega}, \theta\right)\sigma_i^2\chi_i\left(e^{-j\Omega}, \theta\right)d\Omega \tag{B.8}$$

with

$$\zeta\left(z, \theta\right) = \frac{\Delta G(z, \theta)\Gamma(z) + \Delta H(z, \theta)}{H(z, \theta)} \tag{B.9}$$

and

$$\chi_i\left(z, \theta\right) = \frac{\Delta G(z, \theta)}{H(z, \theta)}K_i(z) \tag{B.10}$$

To prove the consistency, we will show that $\theta_0$ is the unique minimiser of (B.8), that is it is the unique parameter vector $\theta^*$ yielding $\overline{E} \ \epsilon_{siso}^2[n, \theta^*] = \sigma_e^2$. We observe that this only holds if $\zeta(z, \theta^*) = \chi_i(z, \theta^*) = 0(i = 1...q)$. Since $q \geqslant 1$ it follows from (B.9) and (B.10) that the latter statement implies that $\Delta G(z, \theta^*) = \Delta H(z, \theta^*) = 0$. This in turn implies $\theta^* = \theta_0$. $\square$

## References

[1] ENTSO-E, Challenges and opportunities Report; 2016.
[2] P.W. Group, Technical Requirements for Frequency Containment Reserve Provision in the Nordic Synchronous Area, Draft, ENTSO-E Nordic; Jun. 2017.
[3] E. Commission, Network code on requirements for grid connection of generators; Apr. 2016. URL https://www.entsoe.eu/network_codes/rfg/.
[4] Jones DI, Mansoor SP, Aris FC, Jones GR, Bradley DA, King DJ. A standard method for specifying the response of hydroelectric plant in frequency-control mode. Electric Power Syst Res 2004;68(1):19–32. https://doi.org/10.1016/S0378-7796(03)00152-4. URL http://www.sciencedirect.com/science/article/pii/S0378779603001524.
[5] Wang J, Su J, Zhao Y, Pang X, Li J, Bi Z. Performance assessment of primary frequency control responses for thermal power generation units using system identification techniques. Int J Electr Power Energy Syst 2018;100:81–90. https://doi.org/10.1016/j.ijepes.2018.02.036. URL http://www.sciencedirect.com/science/article/pii/S014206151732848X.
[6] Hannett LN, Feltes JW, Fardanesh B. Field tests to validate hydro turbine-governor model structure and parameters. IEEE Trans Power Syst 1994;9(4):1744–51. https://doi.org/10.1109/59.331426.
[7] Trudnowski DJ, Agee JC. Identifying a hydraulic-turbine model from measured field data. IEEE Trans Energy Convers 1995;10(4):768–73. https://doi.org/10.1109/60.475851.
[8] Saarinen L, Norrlund P, Lundin U. Field measurements and system identification of three frequency controlling hydropower plants. IEEE Trans Energy Convers 2015;30(3):1061–8. https://doi.org/10.1109/TEC.2015.2425915.
[9] Jakobsen SH, Uhlen K, Bombois X. Identification of hydro turbine governors using PMU data. 2018 IEEE International Conference on Probabilistic Methods Applied to Power Systems (PMAPS) 2018. p. 1–6. https://doi.org/10.1109/PMAPS.2018.8440273.
[10] Duong DT, Uhlen K, Løvlund S, Jansson EA. Estimation of hydro turbinegovernor's transfer function from PMU measurements. In: IEEE PES General Meeting, Boston: IEEE; 2016.

[11] Mogharbel B, Fan L, Miao Z. Least squares estimation-based synchronous generator parameter estimation using PMU data. 2015 IEEE Power Energy Society General Meeting 2015. p. 1–5. https://doi.org/10.1109/PESGM.2015.7286559.

[12] Jakobsen SH, Uhlen K, Lie P. System identification techniques for validating hydro power plant's FCR performance; 2019.

[13] Jakobsen SH, Uhlen K. Testing of a hydropower plant's stability and performance using PMU and control system data in closed loop, IET Generation. Transmiss Distrib 2019. https://doi.org/10.1049/iet-gtd.2019.0804. URL https://digital-library.theiet.org/content/journals/10.1049/iet-gtd.2019.0804.

[14] Jakobsen SH, Uhlen K. Vector fitting for estimation of turbine governing system parameters. 2017 IEEE Manchester PowerTech 2017. p. 1–6. https://doi.org/10.1109/PTC.2017.7980855.

[15] Aghamolki H, Miao Z, Fan L, Jiang W, Manjure D. Identification of synchronous generator model with frequency control using unscented Kalman filter. Electric Power Syst Res 2015;126:45–55. https://doi.org/10.1016/j.epsr.2015.04.016.

[16] Hatziargyriou ND, Karapidakis ES, Stavrakakis GS, Dimopoulos IF, Kalaitzakis K. Identification of synchronous machine parameters using constrained optimization. In: Power Tech Proceedings, 2001 IEEE Porto, vol. 4; 2001, p. 5 pp. vol 4–. doi:10.1109/PTC.2001.964812.

[17] Kosterev D. Hydro turbine-governor model validation in pacific northwest. IEEE Trans Power Syst 2004;19(2):1144–9. https://doi.org/10.1109/TPWRS.2003.821464.

[18] Pantoja JCN, Olarte A, Díaz H. Simultaneous estimation of exciter, governor and synchronous generator parameters using phasor measurements. 2014 Electric

Power Quality and Supply Reliability Conference (PQ) 2014. p. 43–9. https://doi.org/10.1109/PQ.2014.6866781.

[19] Chapman SJ. Electric machinery and power system fundamentals vol. 3. New York: McGraw-Hill; 2002.

[20] Eriksson R, Modig N, Westberg A. FCR-N DESIGN OF REQUIREMENTS, ENTSO-E report, ENTSO-E Nordic; Jul. 2017. URL https://www.statnett.no/for-aktorer-i-kraftbransjen/utvikling-av-kraftsystemet/prosjekter-og-tiltak/nordisk-frekvensstabilitet/.

[21] Ljung L. System identification: theory for the user. 1st ed. Upper Saddle River, NJ, USA: Prentice Hall PTR; 1987.

[22] Mathworks, System Identification Toolbox; 2018. URL https://se.mathworks.com/products/sysid.html.

[23] Working Group on Prime Mover and Energy Supply Models for System Dynamic Performance Studies. Hydraulic turbine and turbine control models for system dynamic studies. IEEE Trans Power Syst. 1992;7(1): 167–179. doi:10.1109/59.141700.

[24] Jakobsen SH, Uhlen K. Development of a test system for identification of turbine dynamics using the dc power flow. IFAC-PapersOnLine 2018;51(2):97–102. https://doi.org/10.1016/j.ifacol.2018.03.017. URL http://www.sciencedirect.com/science/article/pii/S240589631830017X.

[25] Requirements for Instrument Transformers Working, Group. IEEE Standard Requirements for Instrument Transformers, IEEE Std C57.13-2016 (Revision of IEEE Std C57.13-2008) (2016) 1–96Conference Name: IEEE Std C57.13-2016 (Revision of IEEE Std C57.13-2008). doi:10.1109/IEEESTD.2016.7501435.